Hindawi Publishing Corporation
EURASIP Journal on Applied Signal Processing
Volume 2006, Article ID 87298, Pages 1–11
DOI 10.1155/ASP/2006/87298

Use of Genetic Algorithms for Contrast and Entropy Optimization in ISAR Autofocusing

Marco Martorella, Fabrizio Berizzi, and Silvia Bruscoli

Department of Information Engineering, University of Pisa, Via Caruso, 56126 Pisa, Italy

Received 4 May 2005; Revised 25 October 2005; Accepted 21 December 2005

Image contrast maximization and entropy minimization are two commonly used techniques for ISAR image autofocusing. When the signal phase history due to the target radial motion has to be approximated with high order polynomial models, classic optimization techniques fail when attempting to either maximize the image contrast or minimize the image entropy. In this paper a solution of this problem is proposed by using genetic algorithms. The performances of the new algorithms that make use of genetic algorithms overcome the problem with previous implementations based on deterministic approaches. Tests on real data of airplanes and ships confirm the insight.

1. INTRODUCTION

ISAR image reconstruction has been a widely addressed topic in the last few decades [1–4]. The exploitation of large bandwidth signals and the coherent integration of the echoes provide the basis for the ISAR image formation. Before the actual image formation, the signal phase must be compensated in order to remove the target radial movement. We indicate such an operation with "image focusing," and, when no ancillary data are available, with "image autofocusing," because only the received signal is used to perform such an operation.

Among the autofocusing techniques proposed in the literature [5–12], some are based on the use of image focus indicators, such as the image contrast and the image entropy [5–7]. In particular, when the target radial velocity can be approximated with polynomial models, the optimization problems that have to be solved are reduced to a search on a domain of few parameters. In these cases the computational cost is strongly reduced and real-time applications are achievable. Optimization problems have often been solved by using deterministic algorithms such as Steepest Descent, Gradient, Newton and quasi-Newton, Nelder-Mead, and others. Nevertheless, cost functions that have been used as image focus indicators, such as the image contrast and entropy, become highly multimodal when the number of parameters increases. Moreover, deterministic methods can only be applied when the cost function is continuous and differentiable. Recently, optimization algorithms based on a random approach have been introduced in order to overcome the problem of multimodality and differentiability. A subclass of such algorithms is the genetic algorithm (GA).

In this paper we modify two existing autofocusing techniques based on image focus enhancement optimization, namely, the image contrast technique (ICT) and the image entropy technique (IET) by using GAs. Image contrast maximization and image entropy minimization represent two similar optimization problems that encounter the same difficulties when applied to ISAR image autofocusing. Specifically, the high number of local maxima in the cost function causes the convergence of deterministic algorithms to a nonoptimal solution. In [13] a solution based on the use of genetic algorithms for ISAR image autofocusing was proposed in order to improve the joint time-frequency analysis (JTFA) based autofocusing algorithm, which was initially proposed in [11].

In this paper the authors confirm and extend the results obtained in [13] by applying GAs to two well-known autofocusing techniques in order to improve their performances. Real data applications will be shown that demonstrate the effectiveness of GAs when applied to image contrast and entropy based autofocusing techniques.

Section 2 introduces the signal model and the image autofocusing techniques, namely, the ICT and the IET. Section 3 provides a review of classic optimization techniques and introduces the genetic algorithms. Section 4 provides a comparative analysis between classic and genetic optimization techniques when used both in the ICT and IET.

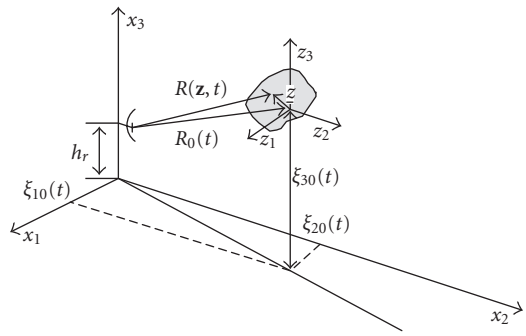

Figure 1: Reference system.

2. SIGNAL MODEL AND AUTOFOCUSING TECHNIQUES

2.1. Signal model

After signal preprocessing [6], the received signal, in free space conditions, can be written in a time-frequency format as follows:

$$S_R(f,t) = W(f,t)e^{-j(4\pi f/c)R_0(t)} \int_V \zeta(z) e^{-j(4\pi f/c)[z^T i_{R_0}^{(z)}(t)]} dz, \tag{1}$$

where $W(f,t) = \text{rect}(t/T_{\text{obs}})\,\text{rect}(f - f_0/B)$ and where f_0 is the carrier frequency, B is the transmitted signal bandwidth, T_{obs} is the observation time, c is the speed of light in free space. Referring to Figure 1, $R_0(t)$ is the modulus of vector $\mathbf{R}_0(\mathbf{t})$ which locates the position of a focusing point on the target, $\mathbf{i}_{\mathbf{R}_0}^{(z)}(t)$ is the unit vector of $\mathbf{R}_0(\mathbf{t})$, $\mathbf{z}$ is the vector that locates a generic point on the target, and V is the spatial region where the reflectivity function $\zeta(z)$ is defined. Function $\text{rect}(x)$ yields 1 when $|x| < 1/2$, 0 otherwise.

When the target does not undergo significant high-speed maneuvers, the distance between the radar and the focusing point can be approximated by its Taylor series expansion around the central time instant $t = 0$:

$$R_0(t) = \sum_{i=0}^{N} \alpha_i t^i, \tag{2}$$

where

$$\alpha_i = \frac{1}{i!}\frac{d^{(i)}}{dt^i} R_0(t)\,|_{t=0}\,. \tag{3}$$

2.2. Autofocusing algorithms

2.2.1. ICT

The ICT attempts to estimate the coefficients of (3) by maximizing the image contrast (IC) with respect to α_i for $i = 1, 2, 3, \ldots, N$. The zero-order term (α_0) can be ignored because it only provokes a range shift in the reconstructed image without producing any defocusing. In the case of an Nth order polynomial phase, the IC can be expressed as follows:

$$\text{IC}(\boldsymbol{\alpha}) = \frac{\sqrt{A\left\{\left[I^2(x_1,x_2;\boldsymbol{\alpha}) - A\{I^2(x_1,x_2;\boldsymbol{\alpha})\}\right]^2\right\}}}{A\{I^2(x_1,x_2;\boldsymbol{\alpha})\}}, \tag{4}$$

where the vector of unknowns can be expressed as $\boldsymbol{\alpha} = [\alpha_1, \ldots, \alpha_N]$, the operator $A(\cdot)$ represents the mean value operator over the image coordinates (x_1, x_2) and where $I(x_1, x_2; \boldsymbol{\alpha})$ is the intensity of the image obtained by compensating the signal with the phase term $e^{j(4\pi f/c)\sum_{i=1}^{N}\alpha_i t^i}$ and by applying a two-dimensional Fourier transform (2D-FT). Analytically, this can be expressed as

$$I(x_1,x_2;\boldsymbol{\alpha}) = 2\text{ D-FT}\left[S_R(f,t)\cdot e^{j(4\pi f/c)\sum_{i=1}^{N}\alpha_i t^i}\right]. \tag{5}$$

Mathematically, the optimization problem can be formulated as follows:

$$(\hat{\boldsymbol{\alpha}}) = \arg\left(\max_{\boldsymbol{\alpha}}\left[\text{IC}(\boldsymbol{\alpha})\right]\right). \tag{6}$$

2.2.2. IET

Equivalently to the ICT, the IET minimizes the image entropy (IE) in order to estimate the coefficients α_i.

By following [7]

$$\text{IE} = -\iint \frac{I^2(x_1,x_2)}{S}\ln\frac{S}{I^2(x_1,x_2)}dx_1\,dx_2, \tag{7}$$

where $S = \iint I^2(x_1,x_2)dx_1\,dx_2$. Therefore, the optimization problem can be written in an mathematical form:

$$(\hat{\boldsymbol{\alpha}}) = \arg\left(\min_{\boldsymbol{\alpha}}\left[\text{IE}(\boldsymbol{\alpha})\right]\right). \tag{8}$$

3. OPTIMIZATION ALGORITHMS

3.1. Deterministic algorithms

Deterministic optimization algorithms, such as Newton, Steepest Descent, Gradient, quasi-Newton, Nelder-Mead [14, 15], are generally efficient methods when the cost function is monomodal and differentiable in the search domain. Often, when the number of variables increases, monomodality is lost and therefore many local minima appear. In such cases, the initial guess that has to be provided as starting point to the search algorithm is essential for the convergence to the global minimum. In this paper, the Nelder-Mead (NM) algorithm [15] has been chosen as a representative of classical methods to compare to genetic algorithms when used to solve problems of IC maximization and IE minimization. The Nelder-Mead algorithm is chosen because it is a more stable and effective algorithm than other classic approaches, such as Newton and Steepest Descent.

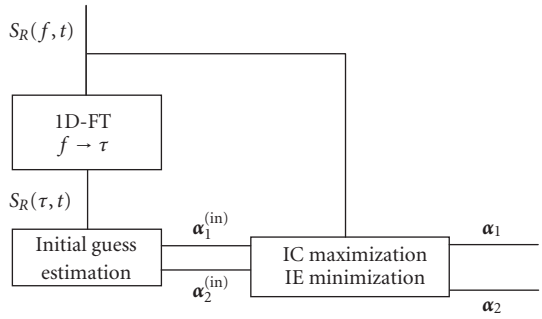

Figure 2: Autofocusing algorithm.

3.2. Genetic algorithms

Genetic algorithms, introduced by Holland in [16], belong to the class of approximation (or heuristic) algorithms, and are largely used to solve optimization problems. The genetic algorithm is a stochastic global search method that mimics the metaphor of natural biological evolution. Whereas traditional search techniques use characteristics of the cost function to determine the next sampling point (e.g., gradients, Hessians, etc.), stochastic search techniques do not need it. In fact, the next solution is determined on the basis of stochastic decision rules, rather than a set of deterministic ones. This peculiarity makes the GAs independent of assumptions like the differentiability of the cost function with respect to the variables that constitute the search domain.

GAs manipulate a family (population) of solutions and implement a "survival of the fittest" strategy to produce better and better approximations of a solution. In general, the fittest individuals of any population tend to reproduce and survive. In this sense the successive generations can improve. Such algorithms are able to solve linear and nonlinear problems by exploring all regions of the search domain and by exponentially exploiting promising areas through mutation, crossover, and selection operations applied to individuals in the population [17].

The crossover operator is used to exchange genetic information between pairs, or larger groups, of individuals. Mutation causes the individual genetic representation to change according to some probabilistic rule (such an operator ensures that there is a nonzero probability of searching a given subspace). This has the effect of inhibiting the possibility to converge to local maxima, rather than to the global maximum.

3.3. Implementation of Nelder-Mead algorithm for IC and IE optimizations

The ICT that makes use of NM technique has been proposed in [5, 6]. In Figure 2, a flow chart of such an algorithm is depicted. The ICT makes use of IC maximization to focus ISAR images. The IET has been derived from the ICT simply by replacing IC maximization with IE minimization. Both algorithms use an initial guess that is estimated by using an initialization technique based on the radon transform (details can be found in [6]). The use of the radon transform has proved to be more efficient than other techniques for estimating the initial guess. The Nelder-Mead algorithm is based on the simplex method for the search of the minimum of a given cost function. Such a method fully described in [15] was implemented in MATLAB by defining two parameters: the maximum number of iterations (MNI) and the tolerance value (TV). The explanation of the former is straightforward and it concerns the stop condition for the iterative algorithm, whereas the second represents the minimum difference allowed between the last two values of the cost function. Also this parameter is used for defining the algorithm stop condition, that is, the algorithm stops iterating when the difference between the last two values of the cost function is smaller than the TV.

3.4. Implementation of genetic algorithms for IC and IE optimizations

The GA replaces both the estimation of the initial guess and the final focusing parameters. In fact, GAs do not need an initial guess. This may represent an additional advantage because the performance of the algorithm is not affected by the estimation of the initial guess. The implementation of the GA used in our analysis is the genetic algorithm optimization toolbox (GAOT) [18], a free toolbox developed at the Department of Industrial and Systems Engineering, North Carolina State University.

The algorithm, implemented in MATLAB, iterates until a stop condition applies. The stop condition can be defined as the MNI or by means of the TV. The MNI is needed in order to control the computational load (CL). Because real time ISAR image reconstruction is often needed, the CL is a parameter to be kept as small as possible. At each iteration the population size (PS) is kept constant by equalling the number of discarded elements to the number of new elements. The elements are discarded by comparing the values of the IC, which represents the "fitness" function. The new elements are generated by "cloning," "combining," and "mutating" the surviving elements (remaining after the discard process). The operation of cloning is performed by choosing the most fit elements (with the largest IC or smallest IE) and copying them into the next generation set. The operation of combining is obtained by choosing two elements within the survivors and by genetically combining them. The genetic combination is a numerical operation that can be performed in many ways [16, 17]. When complex numbers are used, the number representation adopted is the floating point. In this case, an operation called *simple crossover* is performed [17]. A simple crossover consists of:

(1) dividing the binary representation of N elements into two strings of digits of length r and N-r;
(2) concatenating the r digits of the first element with the N-r digits of the second element to create a new element;
(3) concatenating the r digits of the second element with the N-r digits of the first element to create another new element.

Therefore two elements are created from two old elements. The operation of mutating is performed by choosing one or more digits of the binary representation of one element and replacing them with the relative complement values (e.g., $X0X10X$ becomes $X1X01X$). The fittest element of the last generation represents the solution of the optimization problem. Several parameters can be defined [18] in order to implement "ad hoc" genetic algorithms. It is worth mentioning the most significant:

(i) population size,
(ii) number of iterations,
(iii) gene encoding and length,
(iv) selection operation,
(v) crossover and mutation operations.

For what concerns the experiments carried out in section 4, some parameters were kept fixed whereas others were changed in order to find an optimal trade-off between maximum search accuracy and computational cost in a heuristic sense. Specifically, the gene encoding chosen was a floating point binary representation on 64 bits. The selection operation used was the *tournament selection*. The crossover and mutation operations adopted were the *heuristic cross-over* and the *multi-nonuniform mutation*, respectively (see [18] for more details). The population size (PS) is kept constant throughout the generations. Therefore, the initial population size and PS coincide. The PS plays an important role in the effectiveness of the genetic algorithm and a fine tuning is needed in order to improve the optimization performance. The same can be said about the number of iterations, which is defined as the number of iterations that are needed to obtain the solution of the optimization problem. In order to limit the number of iterations the MNI has to be defined. The larger the value of the MNI, the more accurate the solution is, although at the expenses of the computational load, which is linearly proportional to it. A few experiments were run in order to provide suitable values for both the PS and the MNI for the effective application of genetic algorithms to ISAR image autofocusing. The results showed optimal solutions (in a heuristic sense) when PS = 50 and MNI = 50 for a second-order signal phase model and PS = 100 and MNI = 100 for a third-order signal phase model. Such values have been used in the experiments shown in Section 4.

4. PERFORMANCE ANALYSIS

4.1. Data set

The two data sets that are considered for the performance analysis are relative to an aircraft (737, see Figure 3) and a ship (Bulk Carrier, see Figure 4). Details about the radar parameters for the two data sets can be found in Tables 1 and 2, respectively. All data sets were collected by using a low-power instrumented radar system developed by the Australian defence science and technology organisation (DSTO). In particular, the first data has been gathered by using a ground-based radar, located near the Adelaide civilian airport, whereas the second data set has been acquired by an airborne radar. In this second configuration, both the airplane and ship movements contribute to the total aspect angle variation.

Figure 3: Boeing 737.

Figure 4: Bulk Carrier photo.

In this section the effectiveness of the use of genetic algorithms for ISAR image autofocusing is tested by means of real data. Both the ICT and the IET will be considered to validate the proposed solution for a generic parametric technique that makes use of iterative solutions. Moreover, in order to investigate different ISAR scenarios we have chosen two data sets concerning two different radar-target geometries and dynamics. The algorithm performances will be tested by means of three parameters and an image visual inspection. The three parameters are the IC, IE, and CL (as defined in Section 3).

4.2. Test description

The two data sets are analyzed considering both short and long observation times. The longer is the observation time, the higher is the model order that is able to fit the focusing point phase history. We will show that when the integration

Table 1: Radar parameters (aircraft).

N° of sweeps	512
N° of transmitted frequencies	128
Lowest frequency	9.26 GHz
Frequency step	1.5 MHz
Range resolution	0.78 m
Radar height (h_r)	Ground level
Target type	Boeing 737
PRF/sweep rate	20 kHz/156.25 Hz

Table 2: Radar parameters (ship).

N° of sweeps	256
N° of transmitted frequencies	256
Lowest frequency	9.16 GHz
Frequency step	0.6 MHz
Range resolution	0.98 m
Radar height (h_r)	305 m
Target type	Bulk Loader
PRF/sweep rate	20 kHz/78.13 Hz

time is short, the second-order model is able to represent the phase history. The IC generally shows a quite regular behavior when it is a function of two parameters ($\mathrm{IC}(\hat{\alpha}_1, \hat{\alpha}_2)$), as illustrated in Figure 5. In such a case, the NM algorithm is able to solve the optimization problem and find the global maximum. When a long observation time is used to reconstruct the ISAR image, at least a third-order model is required. The introduction of the third parameter causes irregularity in the IC which becomes highly multimodal. In Figure 6, a section of the $\mathrm{IC}(\hat{\alpha}_1, \hat{\alpha}_2, \hat{\alpha}_3)$ along the third-order parameter ($\hat{\alpha}_3$) is illustrated. The presence of many local maxima is clearly visible. In such a case, the NM fails, as the following results will show, whereas the GA provides a successful image autofocusing.

4.3. Test results

4.3.1. Visual inspection

The visual inspection simply consists of a comparison of ISAR images obtained from the same data by means of the deterministic and genetic algorithms. The ISAR images relative to the Boeing 737 data, obtained by means of the GA and the NM are shown, respectively, in Figures 7 and 8. The two images, reconstructed by coherently processing 128 sweeps (0.8 s), show the same features and are equally well focused. The signal phase model used in this case was a second-order polynomial because of the short integration time. As expected, the results obtained with NM and GA are quite comparable. This is due to the fact that the NM algorithm represents a good optimization algorithm for the 2D search

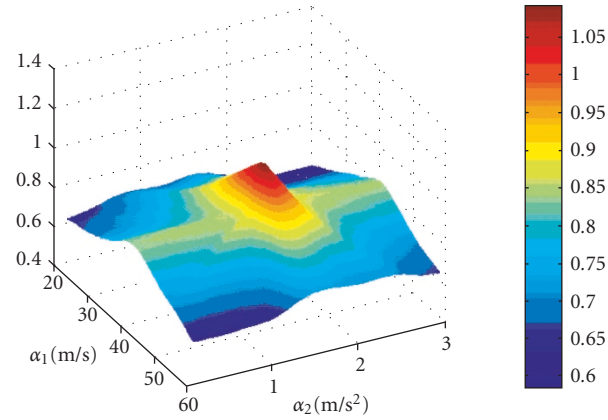

Figure 5: Image contrast.

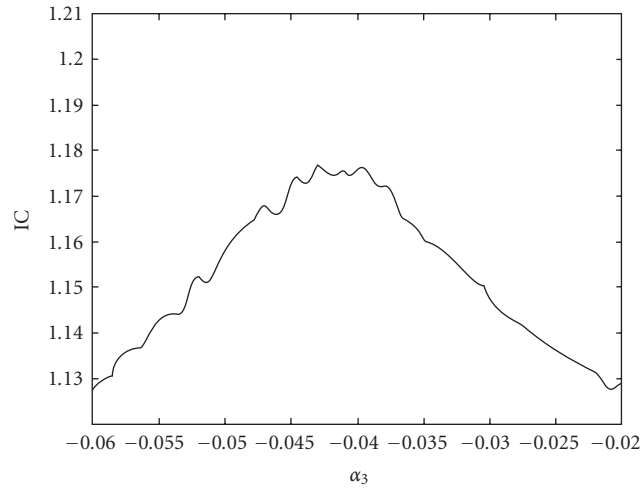

Figure 6: Image contrast section (third-order term).

space represented by the signal phase parameters. The ISAR images shown in Figures 9 and 10 are obtained by coherently processing 512 sweeps (3.2 s) by means of the GA and the NM, respectively. In this case, it is clearly noticeable that the ISAR image, obtained by means of the NM approach, is defocused, whereas the ISAR image relative to the GA shows a good focus. Because of the long integration time, a third order polynomial model was assumed. The results show that the NM algorithm is not able to provide a good image focus whereas the GA is able to find an accurate solution. It is worth noting that in all the cases the NM iteration termination was due to the TV and not to the MNI. This confirms that the NM algorithm converges to local maxima instead of the global maximum.

In order to verify that a second-order model is not accurate enough to represent the signal phase history, we show the ISAR images relative to the long integration time (512×128). Such images were processed by using a second-order model

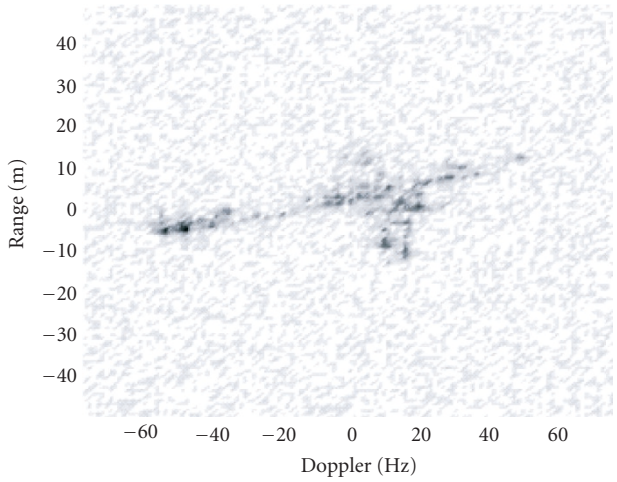

Figure 7: ICT-GA—128 × 128 focused with a second-order model—Boeing 737.

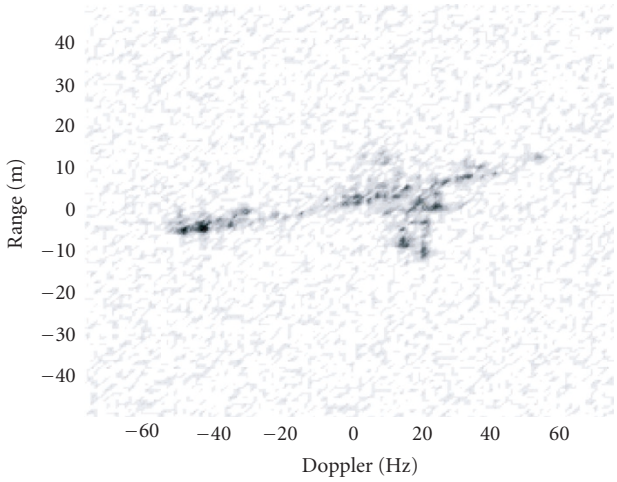

Figure 8: ICT-NM—128 × 128 focused with a second-order model—Boeing 737.

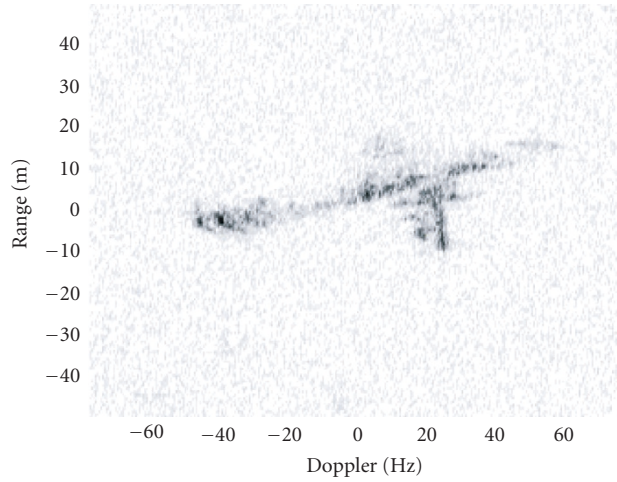

Figure 9: ICT-GA—512 × 128 focused with a third-order model—Boeing 737.

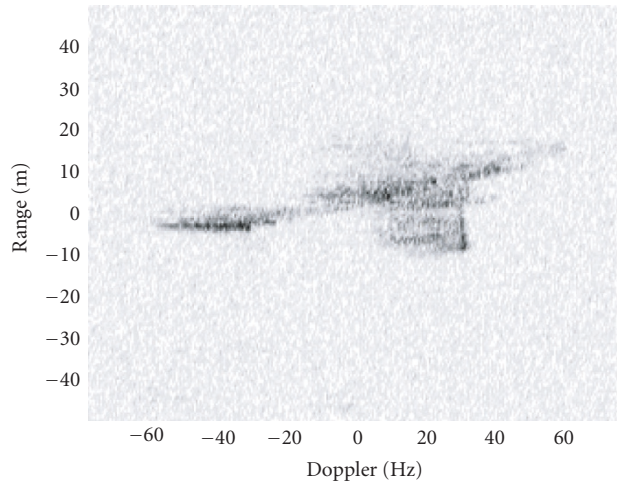

Figure 10: ICT-NM—512 × 128 focused with a third-order model—Boeing 737.

for both the GA and the NM and are shown in Figures 11 and 12, respectively. The image defocus due to the inaccuracy of the second-order model is clearly visible in both images.

The same data set has been used to conduct an equivalent experiment by using the IET. Figures 13, 14 show the ISAR images relative to a short integration time and processed by using a second-order model by means of genetic and deterministic algorithms, respectively. Also in this case both approaches achieve the same result. In Figures 15 and 16, the ISAR images relative to the long integration time are shown. In this case, the use of a third-order model affects negatively the results when a deterministic approach is used, whereas the use of GAs provides a well-focused image.

The second experiment has been conducted for the second data set relative to a Bulk Carrier. In this case only a long observation time (3.2 s) has been considered in order to test the use of a third-order model. Figures 17 and 18 show the two ISAR images obtained by using the GA and the NM, respectively. It is clear that the image focused by means of GAs (Figure 17) is well focused whereas the image obtained by means of NM (Figure 18) is not focused at all.

4.3.2. *Image contrast*

The IC is an indicator of the image focusing: the higher the IC, the better the image focusing. In Table 3 we report the IC

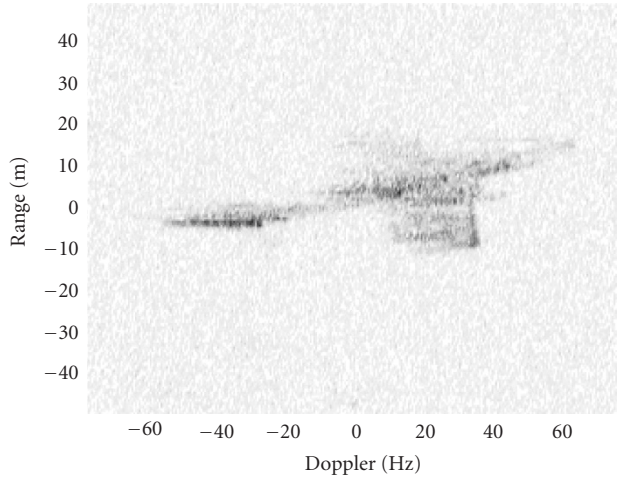

Figure 11: ICT-GA—512 × 128 focused with a second-order model—Boeing 737.

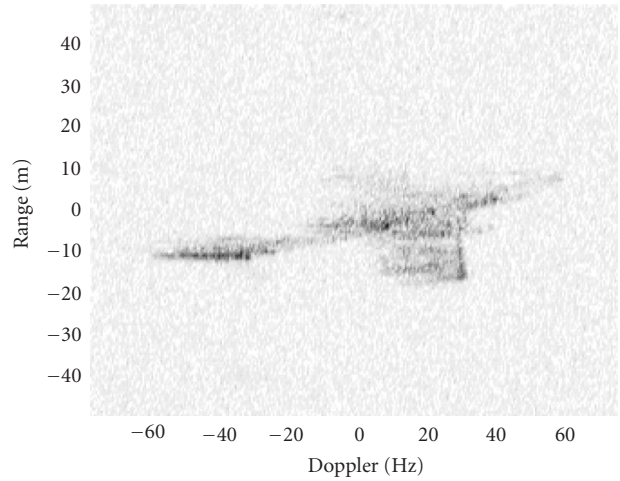

Figure 12: ICT-NM—512 × 128 focused with a second-order model—Boeing 737.

for the ISAR images obtained by processing the two data sets. The results confirm the visual analysis. In particular, we note that a third-order model is needed for longer integration times as confirmed by the image contrast increase. Moreover, the use of GAs is necessary in order to ensure the convergence of the solution to the global maximum, as shown by comparing the IC values in the case of NM and GA, regardless of the particular ISAR autofocusing technique used (either ICT or IET). It is worth noting that small differences in the IC can provoke big differences in the image focus (compare with visual inspection).

4.3.3. Image entropy

The IE is an indicator of the image focus as well as the IC. In this case the smaller the entropy, the better the image focus [6]. In Table 4, the results relative to the IE confirm the results found in both the visual inspection and the IC analysis.

4.3.4. Image peak

The image peak (IP) is another indicator of the image focusing. Its definition is as follows:

$$\mathrm{IP} \triangleq \max\{I^2(x_1, x_2)\}. \tag{9}$$

When an image of a rigid body is well focused, the energy relative to any single scatterer is more concentrated around its peak. Such an indicator of performance could be misleading when used alone but it is a good indicator when it is used jointly with other indicators such as IC and IE, which consider the whole image focus quality. In Table 5, the results relative to the image peak (in dB) strengthen the previous analyses in most of the cases. It is worth noting that the values relative to the Bulk Carrier data set, when the IET-GA is used, show a different trend with respect to the other experiments. In particular the value relative to the second-order and 64 × 256 data set is significantly larger than any other values. This behavior can be explained by the fact that a single scatterer can be highly focused even though the rest of the image is not highly focused. This phenomenon occurs especially when low-order polynomial models are sued for representing the signal phase.

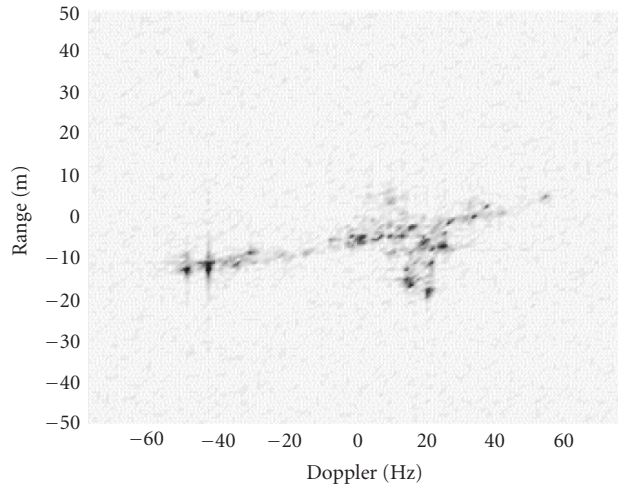

Figure 13: IET-GA—128 × 128 focused with a second-order model—Boeing 737.

4.3.5. Computational load

The CL has been calculated by running the algorithm on a Pentium III—833 MHz processor with 192 MB of RAM, and it is reported in seconds. It is worth noting that the algorithm is coded in MATLAB and it is not optimized, hence only a comparative analysis must be considered. In order to speed

Table 3: Image contrast as indicator of image quality (higher values indicate better image focus).

Algorithm	Model order	Airplane		Bulk Carrier	
		128 × 128	512 × 128	64 × 256	256 × 256
ICT-NM	(2nd order)	**1.27**	1.09	2.84	2.61
	(3rd order)	**1.27**	1.09	2.87	2.60
ICT-GA	(2nd order)	**1.27**	1.09	3.03	2.65
	(3rd order)	**1.27**	**1.18**	**3.05**	**2.92**
IET-NM	(2nd order)	1.26	1.08	2.97	2.65
	(3rd order)	1.25	1.09	2.82	1.48
IET-GA	(2nd order)	1.26	1.07	3.02	2.65
	(3rd order)	**1.27**	1.15	3.02	**2.92**

Table 4: Image entropy as indicator of image quality (lower values indicate better image focus).

Algorithm	Model order	Airplane		Bulk Carrier	
		128 × 128	512 × 128	64 × 256	256 × 256
ICT-NM	(2nd order)	7.10	9.28	6.33	10.63
	(3rd order)	7.10	9.28	6.38	10.62
ICT-GA	(2nd order)	7.10	9.29	6.33	7.57
	(3rd order)	7.09	8.87	**6.17**	7.56
IET-NM	(2nd order)	6.99	9.28	6.33	10.63
	(3rd order)	6.99	9.27	6.37	10.62
IET-GA	(2nd order)	6.99	9.27	6.33	7.56
	(3rd order)	**6.97**	**8.79**	**6.17**	**7.55**

Table 5: Image peak as indicator of image quality expressed in dB scale (higher values indicate better image focus).

Algorithm	Model order	Airplane		Bulk Carrier	
		128 × 128	512 × 128	64 × 256	256 × 256
ICT-NM	(2nd order)	42.1	41.7	55.8	58.7
	(3rd order)	42.1	41.7	54.5	58.8
ICT-GA	(2nd order)	42.0	41.6	56.1	58.1
	(3rd order)	41.9	**46.3**	55.7	57.2
IET-NM	(2nd order)	43.2	41.4	56.4	58.2
	(3rd order)	42.6	41.4	55.8	54.9
IET-GA	(2nd order)	43.2	42.6	**62.4**	58.2
	(3rd order)	**43.4**	**46.3**	56.4	**59.9**

Table 6: CL-time required to find the solution of the optimization problem (in seconds).

Algorithm	Model order	Airplane		Bulk Carrier	
		128 × 128	512 × 128	64 × 256	256 × 256
ICT-NM	(2nd order)	**4.1**	14.1	4.4	**17.8**
	(3rd order)	6.9	30.0	12.8	76.3
ICT-GA	(2nd order)	10.9	63.7	6.7	26.9
	(3rd order)	13.0	77.5	24.4	117.2
IET-NM	(2nd order)	12.5	**12.3**	**4.3**	37
	(3rd order)	10.8	182.9	10.4	165.7
IET-GA	(2nd order)	22.6	238.6	41.4	247.1
	(3rd order)	50.4	534.9	52.3	274.8

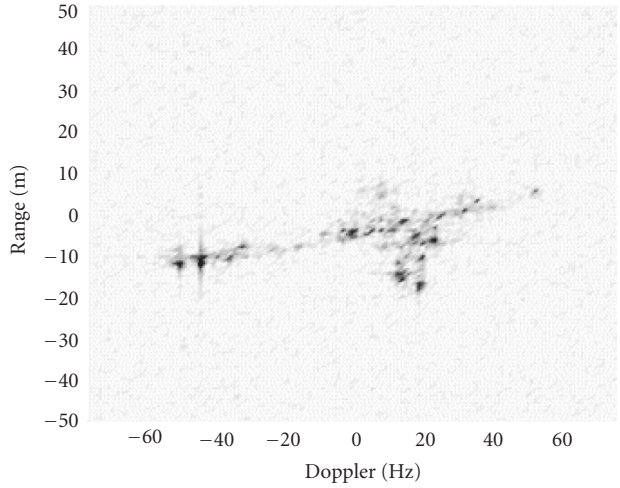

Figure 14: IET-NM—128 × 128 focused with a second-order model—Boeing 737.

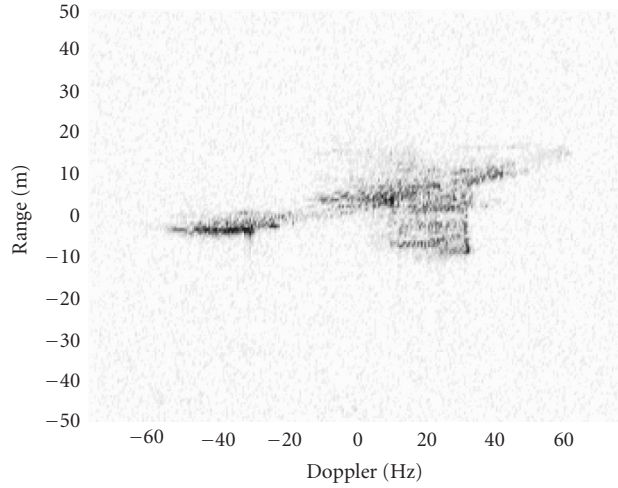

Figure 16: IET-NM—512 × 128 focused with a third-order model—Boeing 737.

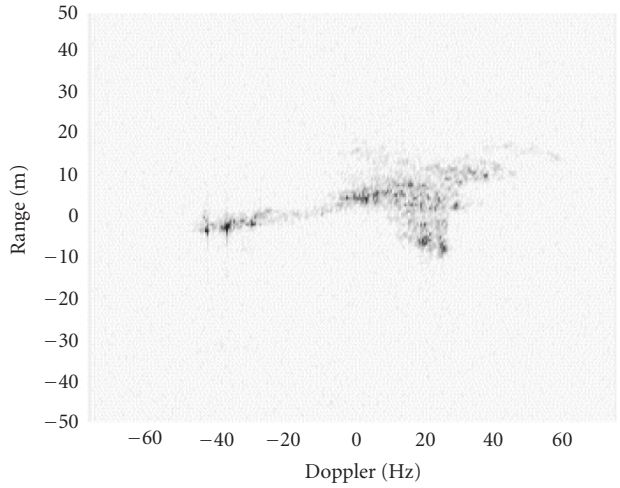

Figure 15: IET-GA—512 × 128 focused with a third-order model—Boeing 737.

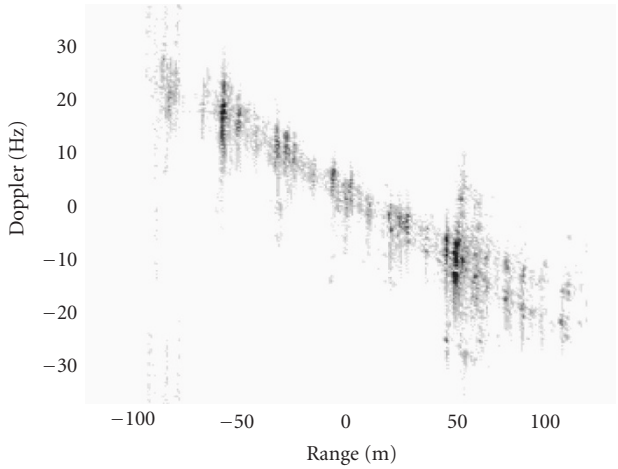

Figure 17: ICT-GA—256 × 256 focused with a third-order model—Bulk Carrier.

up the processing for real-time applications both code optimization and faster processors must be implemented. The results relative to the two data sets are shown in Table 6. The computation burden required by the NM algorithm is generally less than the GA. It is worth noting that such a burden becomes significant when a third-order model is used. Nevertheless, the results obtainable by using GA justify the increase of CL.

5. CONCLUSIONS

In this paper an extension of both the ICT and IET is proposed by introducing genetic algorithms. The ability of such algorithms to solve optimization problems in the case of highly multimodal cost functions has been shown by means of real data for two well-known parametric ISAR autofocusing techniques, namely, the ICT and the IET. The improvement is noticed when long integration times are used to form the ISAR image. In fact, in such cases model orders higher than the second must be used and the cost function becomes highly multimodal. Even by using accurate initial guesses, classical techniques are not always able to converge to the global maximum. In our analysis the NM algorithm has been used to represent deterministic approaches. The results have shown an equal performance at short integration times that leads to the use of deterministic techniques because of their

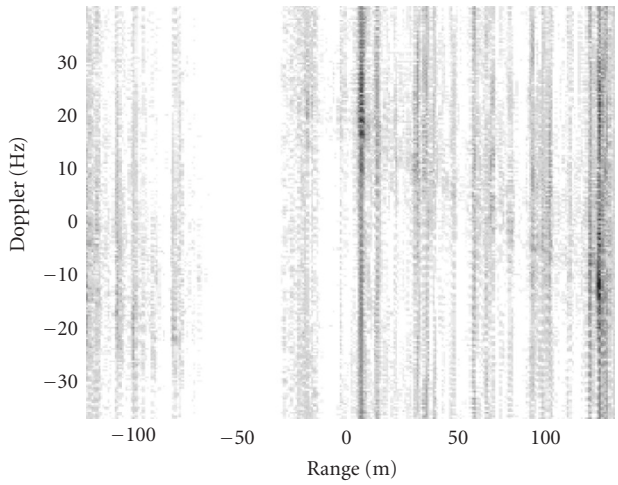

Figure 18: IET-NM—256 × 256 focused with a third-order model—Bulk Carrier.

less expensive computational load. In a generic case, when arbitrary integration times are used, the GA approach shows better performances and robustness, and hence it is preferred to deterministic approaches.

ACKNOWLEDGMENTS

The authors acknowledge the Defense Science and Technology Organisation (DSTO) for the use of real data and the University of North Carolina for sharing the GAOT toolbox. Special thanks to Petrina Kapper for English language support.

REFERENCES

[1] J. L. Walker, "Range-doppler imaging of rotating objects," *IEEE Transactions on Aerospace and Electronic Systems*, vol. 16, pp. 23–52, 1980.

[2] D. A. Ausherman, A. Kozma, J. L. Walker, H. M. Jones, and E. C. Poggio, "Developments in radar imaging," *IEEE Transactions on Aerospace and Electronic Systems*, vol. 20, no. 4, pp. 363–400, 1984.

[3] W. C. Carrara, R. S. Goodman, and R. M. Majewsky, *Spotlight Synthetic Aperture Radar: Signal Processing Algorithms*, Artech House, Boston, Mass, USA, 1995.

[4] D. R. Wehner, *High Resolution Radar*, Artech House, Norwood, Mass, USA, 1995.

[5] F. Berizzi and G. Corsini, "Autofocusing of inverse synthetic aperture radar images using contrast optimisation," *IEEE Transaction on Aerospace and Electronic System*, vol. 32, no. 3, pp. 1185–1191, 1996.

[6] M. Martorella, B. Haywood, F. Berizzi, and E. Dalle Mese, "Performance analysis of an ISAR contrast based autofocusing algorithm using real data," in *Proceedings of IEE Radar Conference*, pp. 200–205, Adelaide, Australia, September 2003.

[7] L. Xi, L. Giosui, and J. Ni, "Autofocusing of ISAR images based on entropy minimisation," *IEEE Transactions on Aerospace and Electronic Systems*, vol. 35, no. 4, pp. 1240–1252, 1999.

[8] B. Haywood and R. J. Evans, "Motion compensation for ISAR imaging," in *Proceedings of the IEEE Australian Symposium on Signal Processing and Applications (ASSPA '89)*, pp. 113–117, Adelaide, Australia, April 1989.

[9] J. Li, R. Wu, and V. C. Chen, "Robust autofocus algorithm for ISAR imaging of moving targets," *IEEE Transactions on Aerospace and Electronic Systems*, vol. 37, no. 3, pp. 1056–1069, 2001.

[10] W. Haiqing, D. Grenier, G. Y. Delisle, and F. Da-Gang, "Translational motion compensation in ISAR image processing," *IEEE Transactions on Image Processing*, vol. 4, no. 11, pp. 1561–1571, 1995.

[11] Y. Wang, H. Ling, and V. C. Chen, "ISAR motion compensation via adaptive joint time-frequency technique," *IEEE Transactions on Aerospace and Electronic Systems*, vol. 34, no. 2, pp. 670–677, 1998.

[12] I.-S. Choi, B.-L. Cho, and H.-T. Kim, "ISAR motion compensation using evolutionary adaptive wavelet transform," *IEE Proceedings on Radar, Sonar and Navigation*, vol. 150, no. 4, pp. 229–233, 2003.

[13] J. Li and H. Ling, "Use of genetic algorithms in ISAR imaging of targets with higher order motions," *IEEE Transactions on Aerospace and Electronic System*, vol. 39, pp. 343–351, 2002.

[14] E. Polak, *Optimization: Algorithms and Consistent Approximations*, vol. 124 of *Applied Mathematical Sciences*, Springer, New York, NY, USA, 1997.

[15] J. A. Nelder and R. Mead, "A simplex method for function minimisation," *Computer Journal*, vol. 7, pp. 308–313, 1965.

[16] J. Holland, *Adaptation in Natural and Artificial Systems*, University of Michigan Press, Ann Arbor, Mich, USA, 1975.

[17] Z. Michalewicz, *Genetic Algorithms + Data Structures = Evolution Programs*, Springer, New York, NY, USA, 1994.

[18] C. R. Houck, J. A. Joines, and M. G. Kay, "A genetic algorithm for function optimization: a MATLAB implementation," North Carolina State University, http://www.ie.ncsu.edu/mirage/GAToolBox/gaot/.

Marco Martorella was born in Portoferraio (Italy) in June 1973. He received the Telecommunication Engineering Laurea and Ph.D. degrees from the University of Pisa (Italy) in 1999 and 2003, respectively. He became a Postdoctoral Researcher in 2003 and a Permanent Researcher/Lecturer in 2005 at the Department of Information Engineering of the University of Pisa. He joined the Department of Electrical and Electronic Engineering (EEE) of the University of Melbourne during working on his Ph.D., the Department of Electrical and Electronic Engineering (EEE) of the University of Adelaide under a postdoctoral contract, and the Department of Information Technology and Electrical Engineering (ITEE) of the University of Queensland as a Visiting Researcher between 2001 and 2006. His research interests are in the field of synthetic aperture radar (SAR) and inverse synthetic aperture radar (ISAR). He is an IEEE Member since 1999.

Fabrizio Berizzi was born in Piombino, Italy, in 1965. He received the Electronic Engineering "Laurea" and Ph.D. degrees at the University of Pisa (Italy) in 1990 and 1994. Since October 2000 he has been an Associate Professor at the Department of Information Engineering of the University of Pisa (Italy). He currently lectures "numerical communications" in the computer engineering course, "project and simulation of remote sensing systems" in the telecommunication engineering course, and "signal theory and applications" at the Italian Navy. He has published more than 60 scientific papers. Since 1998, he has been the principal investigator of two Italian Space Agency (ASI) projects on sea remote sensing. His research interests are in the fields of radar systems, synthetic aperture radar (SAR and ISAR), sea remote sensing by means of active sensors. He is a Member of IEEE.

Silvia Bruscoli was born in Cecina, Italy, in August 1977. She received the "Laurea" degree in telecommunication engineering at the University of Pisa (Italy), in 2003. She is currently a Ph.D. student in "methods and technologies for environmental monitoring" at the Department of Information Engineering of the University of Pisa. Her research interests include inverse synthetic aperture radar and target classification in SMR environments.